PHYSICAL REVIEW B VOLUME 43, NUMBER 15 15 MAY 1991-II

Brief Reports

Brief Reports are accounts of completed research which, while meeting the usual **Physical Review** *standards of scientific quality, do not warrant regular articles. A Brief Report may be no longer than four printed pages and must be accompanied by an abstract. The same publication schedule as for regular articles is followed, and page proofs are sent to authors.*

Interatomic potential for directional bonding: The rotated-second-moment approximation

Joel D. Kress and Arthur F. Voter
Theoretical Division (T-12, MS B268), Los Alamos National Laboratory, Los Alamos, New Mexico 87545

(Received 1 November 1990; revised manucript received 11 March 1991)

An interatomic potential is presented, the rotated-second-moment approximation (RSMA), which incorporates directional bonding through energy moments evaluated over directional atomic orbitals. When nondirectional orbitals are used, RSMA reduces to the standard SMA (which is equivalent to the embedded-atom method), and is thus capable of describing metallic systems. A model RSMA potential is constructed for 3*d* transition metals, with only first-neighbor shell interactions, which can correctly predict the experimental trend in the relative stability of the fcc and hcp structures.

The crucial ingredient for obtaining meaningful properties from an atomistic simulation is an accurate interatomic potential.[1] Excellent interatomic potentials do exist for certain classes of materials. For metallic systems, the embedded-atom method[2] (EAM), and the equivalent second-moment approximation[3] (SMA), work well for fcc metals, alloys of fcc metals, and some bcc metals. For covalent systems which are dominated by directional bonding, a different approach is required. The majority of potentials for covalent systems rely on three-body terms that depend explicitly on the experimentally observed bond angles, an approach that does not treat different crystal structures on an equal footing, and usually lacks flexibility. What would be highly desirable is a form of interatomic potential that embodies more of the physics and chemistry of directional bonding, can describe both metallic and covalent systems, is easily transferable to new materials and alloys, and is feasible for molecular dynamics (MD).

Driven by considerations such as these, a few workers have recently proposed more advanced potential forms. Baskes *et al.*[4] constructed Si and Ge potentials using the EAM augmented by an angle-dependent density term. Moriarty[5] derived a potential for Mo that maps a density-functional formalism onto three- and four-body radial and angular terms. Pettifor has proposed a bond-order potential[6] based on approximations to tight-binding theory. Carlsson *et al.*[7] developed the generalized embedded-atom format (GEAF), which is discussed below. Other examples also exist.[1]

We present here the rotated-second-moment approximation (RSMA), which incorporates directional bonding through energy moments evaluated over atomic orbitals. When nondirectional (*s*-type) orbitals are used, RSMA reduces to the SMA, and is thus capable of describing metallic crystals as well. In the following, RSMA is derived from intuitive quantum-chemical principles, and is then shown to correspond to a well-defined approximation to the tight-binding recursion method.[8] A model RSMA potential is then constructed for 3*d* transition metals. The experimental trend in the relative stability of the fcc and hcp structures is correctly predicted with only the first neighbor shell.

We begin by expressing the total energy of a material as[9]

$$E_{\text{tot}}^{\text{RSMA}} = E_{\text{bond}} + E_{\text{pair}} = \sum_i E_{\text{bond},i} + \tfrac{1}{2}\sum_i \sum_{j(\neq i)} \phi(r_{ij}) \;. \tag{1}$$

(Throughout, sums over Roman indices are sums over atoms). $E_{\text{bond},i}$ is the bonding energy contribution due to atom *i*. $\phi(r_{ij})$ is a pairwise potential, a function of the internuclear distance $r_{ij}=|\mathbf{r}_{ij}|$, representing core-core interactions and neglected contributions to the true bonding energy (such as double counting terms). The bonding energy is defined as[10]

$$E_{\text{bond},i} = \int_{-\infty}^{E_F} \varepsilon n_i(\varepsilon)\,d\varepsilon \;, \tag{2}$$

where $n_i(\varepsilon)$ is the density of states (DOS) projected onto atom *i*. The Fermi energy E_F is found from

$$N_{\text{val}} = \int_{-\infty}^{E_F} n_i(\varepsilon)\,d\varepsilon \;, \tag{3}$$

where N_{val} is the number of valence electrons on atom *i*.

Obtaining the exact shape of the DOS would require solving the many-electron problem for the material. The RSMA method approximates the shape of the DOS from its first two energy moments. The mth moment,

$$\mu_{mi}=\int_{-\infty}^{\infty}\varepsilon^m n_i(\varepsilon)d\varepsilon \ , \tag{4}$$

can be computed[11,12] for orbital $|i,\alpha\rangle$ within a one-electron tight-binding approximation,

$$\mu_{mi\alpha}=\langle i,\alpha|\hat{H}^m|i,\alpha\rangle \ , \tag{5}$$

where $\alpha=1,\ldots,n_{\text{orb}}$, is the angular momentum index $(s,p_x,\ldots,d_{xy},\ldots)$. The energy of $|i,\alpha\rangle$ for an isolated atom is $\varepsilon^0_{i,\alpha}$.

Upon insertion of a complete set of orbitals, the second moment for orbital α is

$$\mu_{2i\alpha}=\sum_{j(\neq i)}\sum_{\beta}\langle i,\alpha|\hat{H}|j,\beta\rangle\langle j,\beta|\hat{H}|i,\alpha\rangle \ . \tag{6}$$

(Throughout, sums over Greek indices are sums over n_{orb} orbitals). The hopping integral matrix elements in Eq. (6) are assumed to have a two-center form; the radial dependencies are parametrized and the angular dependencies are determined by the Slater-Koster relations.[13]

The total DOS for atom i is constructed as a sum over contributions from each orbital

$$n_i(\varepsilon)=N\sum_{\alpha} n_{i\alpha}(\mu_{1i\alpha},\mu_{2i\alpha},\varepsilon) \ , \tag{7}$$

where $n_{i\alpha}$ is normalized to unit area and $N\ (\equiv\mu_{0i\alpha})=2$ is the number of electrons in a full orbital (spin is neglected). $\mu_{1i\alpha}$ and $\sqrt{\mu_{2i\alpha}}$ provide the center and "width" of $n_{i\alpha}$, respectively. A few DOS shapes we have considered include a bonding-antibonding pair of dirac δ functions (placed at $\mu_{1i\alpha}\pm\sqrt{\mu_{2i\alpha}}$), a rectangle (the Friedel approximation[14] to a d band), and a Gaussian. Simple shapes for $n_{i\alpha}$ allow an efficient inversion of Eq. (3), which, given N_{val}, must be solved for E_F.

If an s-orbital basis is used, the second moment becomes a scalar, $\mu_{2i,s}$. The SMA bonding-energy expression $E_{\text{bond},i}=-\sqrt{\mu_{2i,s}}$ is then derived[11] by neglecting the first moment and using a half-filled Gaussian DOS.

If the first and second moments resulting from a directional (non-s-type) basis are placed directly into Eq. (7), the resulting DOS (and hence the energy) is *not* invariant to rotation of the coordinate system, a fatal flaw. Similar behavior has been observed by Inoue and Ohta[15] in the recursion method. To achieve rotational invariance, the second-moment matrix, defined as

$$[M_{2i}]_{\alpha,\beta}=\sum_{j(\neq i)}\sum_{\gamma}\langle i,\alpha|\hat{H}|j,\gamma\rangle\langle j,\gamma|\hat{H}|i,\beta\rangle \ , \tag{8}$$

is diagonalized ($\underline{M}_{2i}\underline{U}=\underline{U}\,\underline{L}_{2i}$, with $[\underline{L}_{2i}]_{\alpha\alpha}=\lambda_{2i,\alpha}$), and the eigenvalues $\{\lambda_{2i,\alpha}\}$ are employed as the $\mu_{2i,\alpha}$ in Eq. (7). This step provides the crucial rotational invariance of the energy expression. The diagonalization has the effect of *rotating* the orbital basis, with the eigenvalues corresponding to the second moments evaluated in this rotated basis. The desired first-moment matrix elements $\{\mu_{1i\alpha}\}$ can then be computed as the diagonal elements of $\underline{U}^{\dagger}\underline{M}_{1i}\underline{U}$. Looking ahead to MD applications, this rotation of $\underline{M}_{1i}$ complicates the calculation of $dE_{\text{bond},i}/d\mathbf{r}_{ij}$, because the derivatives of $\underline{U}$ cannot be evaluated analytically. To avoid this, we now make the approximation that $\underline{M}_{1i}$ and $\underline{M}_{2i}$ have the same eigenvectors. This is true by symmetry for fcc and ideal hcp lattices, but not for arbitrarily distorted geometries. Given this assumption, the first-moment eigenvalues can be expressed as a function of the second-moment eigenvalues,

$$\lambda_{1i,\alpha}=f_{21}(\lambda_{2i,\alpha})+g_{21}(\bar{\lambda}_{2i}) \ , \tag{9}$$

where $\bar{\lambda}_{2i}=\text{Tr}[\underline{M}_{2i}]/n_{\text{orb}}$.

The steps for calculating a RSMA bonding energy for atom i can be summarized as follows. First, the orbital basis, the DOS shape, and the form for the radial hopping integrals are specified. Then, to compute $E_{\text{bond},i}$ for a given geometry of neighbors about atom i, (i) construct and diagonalize $\underline{M}_{2i}$, (ii) obtain $\lambda_{1i,\alpha}$ from Eq. (9), (iii) construct the DOS [Eq. (7)], (iv) compute E_F from Eq. (3) for a specified number of electrons (N_{val}), and (v) compute $E_{\text{bond},i}$ from Eq. (2).

The RSMA can also be obtained from a well-defined approximation to the matrix recursion method.[15] Truncating after the first recursion, the DOS on atom i can be expressed[15] as a trace of the Green's-function matrix (resolvent)

$$\begin{aligned} n_i(\varepsilon)&=\text{Tr}\underline{G}_i(\varepsilon)\\ &=\text{Tr}[-(1/\pi)\text{Im}(z\underline{I}-\underline{M}_{1i}-\underline{M}_{2i}/z)^{-1}] \ , \end{aligned} \tag{10}$$

where Im represents the imaginary part, $z=\varepsilon+iE$ as $E\rightarrow 0$, and $\underline{I}$ is a unit matrix of order n_{orb}. In this context, the SMA is derived from Eq. (10) by computing in an s-orbital basis $\underline{M}_{2i}=\mu_{2i,s}$, setting $\underline{M}_{1i}=\mu_{1i,s}=0$, and half filling the resulting DOS, $n_i(\varepsilon)=\delta(\varepsilon+\sqrt{\mu_{2i,s}})+\delta(\varepsilon-\sqrt{\mu_{2i,s}})$.

To compute the DOS from Eq. (10) using directional orbitals, the trace must be properly evaluated using $\underline{M}_{1i}$ and $\underline{M}_{2i}$. Assuming Eq. (9), insertion of the spectral representations of $\underline{M}_{1i}$ and $\underline{M}_{2i}$ into Eq. (10) yields

$$\begin{aligned} n_i(\varepsilon)&=\sum_{\alpha}-(1/\pi)\text{Im}(z-\lambda_{1i,\alpha}-\lambda_{2i,\alpha}/z)^{-1}\\ &=N\sum_{\alpha}N^{+}_{i,\alpha}\delta(\varepsilon-r^{+}_{i,\alpha})+N^{-}_{i,\alpha}\delta(\varepsilon-r^{-}_{i,\alpha}) \ , \end{aligned} \tag{11}$$

where

$$r^{+,-}_{i,\alpha}=\lambda_{1i,\alpha}/2\pm\sqrt{(\lambda_{1i,\alpha}/2)^2+\lambda_{2i,\alpha}} \ , \tag{12a}$$

$$N^{+,-}_{i,\alpha}=\tfrac{1}{2}\pm\tfrac{1}{2}[(\lambda_{1i,\alpha}/2)/\sqrt{(\lambda_{1i,\alpha}/2)^2+\lambda_{2i,\alpha}}] \ , \tag{12b}$$

and $N=2$. The form of Eq. (11) is consistent with Eq. (7) as long as the *rotated* first and second moments are used to parametrize the $n_{i\alpha}(\varepsilon)$. Note that the positioning of the two δ functions in Eq. (11) differs from the bonding-antibonding DOS mentioned above, and the two δ functions now have unequal weights. To compensate for performing only one recursion in generating Eq. (10), it is reasonable to try other forms for the orbital-projected DOS, as discussed above.

Before going on to an application of the RSMA, we discuss the GEAF potential for Si developed by Carlsson *et al.*[7] The GEAF potential contains three types of many-body terms. They derive a second-moment term from Eq. (10) above with (i) $\underline{M}_{2i}$ constructed from an s- and p-orbital basis, (ii) $\underline{M}_{1i}$ neglected, and (ii) a half-full sp^3 band (appropriate for Si). The other two GEAF terms are a dipole term, which depends on the off-diagonal s-p coupling in $\underline{M}_{2i}$, and a fourth-moment term, which depends on the trace and eigenvalues of $\underline{M}_{2i}$ and on the trace of the fourth-moment matrix. In contrast, the RSMA includes both first and second (but not higher) moments.

To demonstrate the RSMA potential, we compute the hcp-fcc stability, $\Delta E(\text{hcp}-\text{fcc})=E_{\text{tot}}(\text{hcp})-E_{\text{tot}}(\text{fcc})$, of $3d$ transition metals using a first-nearest-neighbor (NN) model. Although d metals are not usually considered as directionally bonded materials, the partial occupation of d valence orbitals provides some angular character that augments the overall metallic character. Experimentally, d metals with a nearly empty valence shell are hcp, whereas those with a nearly full valence shell are fcc. An atom in either the fcc or ideal hcp structure has 12 NN's, with the difference between the two structures arising purely from the angular symmetry (O_h for fcc, D_{3h} for hcp). $\Delta E(\text{hcp}-\text{fcc})$ thus depends only on E_{bond}; the pairwise terms cancel. While the SMA (or any centrosymmetric potential) cannot differentiate between the two structures until third NN's, the partially occupied $3d$ shell leads to a difference at the first-NN level if angular effects are included.

The $\langle i,\alpha|\hat{H}|j,\gamma\rangle$ are computed by applying the Slater-Koster relations using the two-center *radial* hopping integrals $dd\sigma$, $dd\pi$, and $dd\delta$. Within a canonical d-band model,[16] $ddm=C_m\frac{2}{5}W(S/r_{ij})^5$ (in the notation of Ref. 9), where $C_\sigma=-6$, $C_\pi=4$, $C_\delta=-1$, S is the Wigner-Seitz radius, and W is an approximate bandwidth.[16] The parameters appropriate for Ni are used,[10] yielding $\frac{2}{5}WS^5=7.57$ eV Å^5. To speed computation, the d-orbital basis on each neighbor (j) is made spherically symmetric by setting $C_\sigma^S=\sqrt{C_\sigma^2+2C_\pi^2+2C_\delta^2}=\sqrt{70}$, $C_\pi^S=0$, $C_\delta^S=0$. (The full d basis is retained on atom i.) The same qualitative results are obtained if the full d basis is used for the neighbors (though smaller fcc-hcp splittings result) or if the parameters[10] from any of the $3d$ metals are employed, where $dd\sigma$ ranges from 0.1 eV for Sc to 0.06 eV for Cu.

From the rotated second moments, the first moments are assigned as $\lambda_{1i,\alpha}=s\lambda_{2i,\alpha}-s\bar{\lambda}_{2i}$ with $s=0.5$, which gives a zero trace of the first moment and is consistent with Eq. (9). The resulting DOS using the rectangle model for $n_{i\alpha}$ is shown in Fig. 1 for both the fcc and hcp structures. Each rectangle is centered at $\lambda_{1i,\alpha}+\varepsilon_{i,\alpha}^0$ with width $\sqrt{12\lambda_{2i,\alpha}}$. The rotated second moments (and the first moments by definition) exhibit O_h and D_{3h} crystal-field splitting patterns[17] for fcc and hcp, respectively, evident on the edges of each DOS.

The trend in the d-band filling is obtained by filling the DOS one electron at a time ($N_{\text{val}}=1,2,\ldots,9$), leading to the $\Delta E(\text{hcp}-\text{fcc})$ values shown in Fig. 2 for the rectangular DOS, Gaussian DOS, and recursion DOS [Eq. (11)]. Assuming a filled $4s$ shell, the rectangular DOS, the Gaussian DOS, and other shapes we have tried each predict the correct trend: hcp is more stable for d^1 and d^2 and fcc is more stable for d^8 and d^9; the stability is qualitatively insensitive to the choice of DOS shape. The SMA model gives a straight line at $\Delta E(\text{hcp}-\text{fcc})=0$. In the middle region of Fig. 2, the bcc phase is most stable experimentally (except for Mn, which exists in a "complex" structure). In this simple model no conclusions can be made about the relative stability of bcc, as it has only eight NN's and thus a different E_{pair}. If the second moments are neglected (equivalent to crystal-field theory[17]), then $\Delta E(\text{hcp}-\text{fcc})=0$ for d^1 and d^2. If the first moments

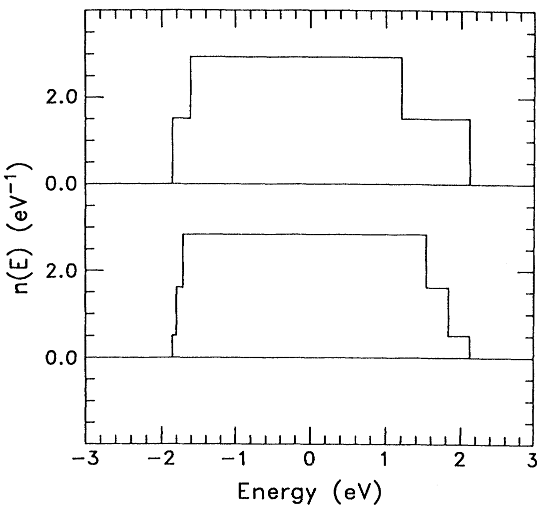

FIG. 1. RSMA density of states (DOS) for nearest-neighbor interactions using the rectangle model for the orbital-projected DOS. Upper plot, fcc; lower plot, hcp.

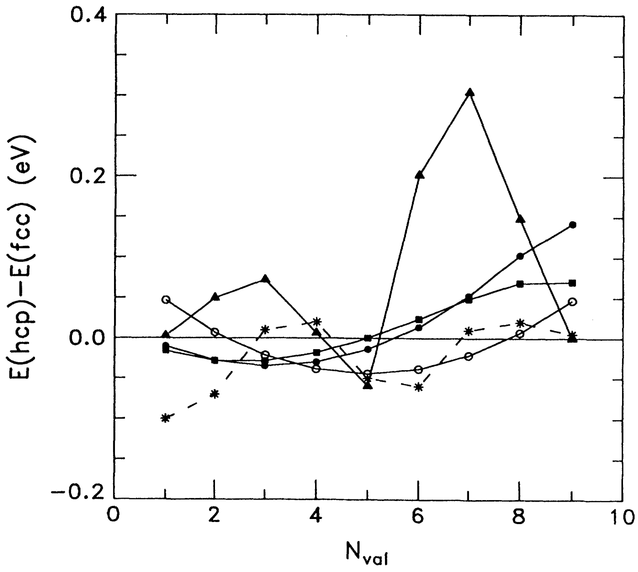

FIG. 2. Energy difference between ideal hcp and fcc structures for nearest-neighbor interactions as a function of d-band filling. Solid circles, rectangular DOS; solid squares, Gaussian DOS; solid triangles, recursion DOS [Eq. (11)]; open circles, rectangular DOS with the first moment set to zero; stars, FP-LMTO results estimated from Fig. 1 of Paxton *et al.* (Ref. 18).

are neglected ($\lambda_{1i\alpha}=0$), the hcp-fcc stability curve (open circles in Fig. 2) is nonzero but exhibits electron-hole symmetry. The first moments thus make it possible to favor one structure for a few d electrons and the other structure for many d electrons; they do *not* simply provide a constant energy shift. Also shown are non-spin-polarized full-potential linear-muffin-tin-orbital (FP-LMTO) results,[18] which display an extra oscillation (as N_{val} is varied) not predicted by the Gaussian or rectangular DOS models. The recursion DOS does show this extra oscillation, although it does not predict the correct hcp-fcc trend. The only free parameter in the present model is s, which is fixed at 0.5 by minimizing $\Delta E(\mathrm{hcp}-\mathrm{fcc})$ for d^1; other values for s give the same trend.

The ability of the RSMA to distinguish fcc from hcp at first NN's using only first- and second-moment information is perhaps unexpected. Ducastelle and Cyrot-Lackmann[12] showed that the first nonidentical traced mth moment, $\mathrm{Tr}[\underline{M}_{m,i}]$, is $m=4$ for the two structures, and Glanville *et al.*[19] showed that $\mathrm{Tr}[\underline{M}_{5,i}]$ is needed to find converged agreement in the hcp/fcc trend using the recursion method. We find that the second moment is sufficient to distinguish hcp from fcc when the *whole* matrix is used. Moreover, the first moment, which is usually neglected in approximations to tight binding, can provide the desired electron-hole asymmetry.

In conclusion, the RSMA potential incorporates directional bonding through the use of directional orbitals (the valence orbitals for the element of interest), rather than fitting to explicit angles, and contains the highly successful SMA as a subset. Parametrization can be effected through the radial shape of the hopping integrals and ϕ, the form of Eq. (9), and the shape of the DOS. Chemical trends can be determined by varying the number of valence electrons N_{val}. The extension to heteronuclear materials, including mixed covalent-metallic systems, should be straightforward.

It is a pleasure to acknowledge useful discussions with Ross Underhill, David Pettifor, Jeff Hay, and Shao Ping Chen. This work was performed under the auspices of the U.S. Department of Energy and was partially supported by the Center for Materials Science at Los Alamos.

---

[1] *Atomistic Simulation of Materials–Beyond Pair Potentials,* edited by V. Vitek and D. J. Srolovitz (Plenum, New York, 1989).

[2] M. S. Daw and M. I. Baskes, Phys. Rev. Lett. **50**, 1285 (1983); Phys. Rev. B **29**, 6443 (1984).

[3] M. W. Finnis and J. E. Sinclair, Philos. Mag. A **50**, 45 (1984).

[4] M. I. Baskes, Phys. Rev. Lett. **59**, 2666 (1987); M. I. Bakses, J. S. Nelson, and A. F. Wright, Phys. Rev. B **40**, 6085 (1989).

[5] J. A. Moriarty, Phys. Rev. B **42**, 1609 (1990).

[6] D. G. Pettifor, Phys. Rev. Lett. **63**, 2480 (1990).

[7] A. E. Carlsson, P. A. Fedders, and C. W. Myles, Phys. Rev. B **41**, 1247 (1990).

[8] R. Haydock, V. Heine, and M. J. Kelly, J. Phys. C **8**, 2591 (1975). See also the entire volume 35 of *Solid State Physics,* edited by H. Ehrenreich, F. Seitz, and D. Turnbull (Academic, New York, 1980).

[9] A. P. Sutton, M. W. Finnis, D. G. Pettifor, and Y. Ohta, J. Phys. C **21**, 35 (1988).

[10] W. A. Harrison, *Electronic Structure and the Properties of Solids* (Freeman, San Francisco, 1980).

[11] F. Cyrot-Lackmann, J. Phys. Chem. Solids **29**, 1235 (1968).

[12] F. Ducastelle and F. Cyrot-Lackmann, J. Phys. Chem. Solids **32**, 285 (1971).

[13] J. C. Slater and G. F. Koster, Phys. Rev. **94**, 1498 (1954).

[14] J. Friedel, *Physics of Metals,* edited by J. M. Ziman (Pergamon, London, 1969), Chap. 8.

[15] J. Inoue and Y. Ohta, J. Phys. C **20**, 1947 (1987).

[16] O. K. Andersen, Phys. Rev. B **12**, 3060 (1975).

[17] B. N. Figgis, *Introduction to Ligand Fields* (Wiley, New York, 1966).

[18] A. T. Paxton, M. Methfessel, and H. M. Polatoglou, Phys. Rev. B **41**, 8127 (1990). The experimental (not ideal) c/a was used for hcp.

[19] S. Glanville, A. T. Paxton, and M. W. Finnis, J. Phys. F **18**, 693 (1988).